International Journal of Nanomedicine

Dovepress
open access to scientific and medical research

Open Access Full Text Article

ORIGINAL RESEARCH

# Mixed micelles loaded with the 5-benzylidenethiazolidine-2,4-dione derivative SKLB023 for efficient treatment of non-alcoholic steatohepatitis

This article was published in the following Dove Press journal:
*International Journal of Nanomedicine*



Yanping Li[1]
Ting Zhang[2]
Qinhui Liu[1]
Jinhang Zhang[1]
Rui Li[1]
Shiyun Pu[1]
Tong Wu[1]
Liang Ma[3]
Jinhan He[1]

[1]Laboratory of Clinical Pharmacy and Adverse Drug Reaction, [2]Department of Pharmacy, [3]Division of Nephrology, Kidney Research Institute, Collaborative Innovation Center of Biotherapy, West China Hospital of Sichuan University, Chengdu 610041, People's Republic of China

**Background:** SKLB023, a novel 5-benzylidenethiazolidine-2,4-dione based-derivative, specifically inhibits inducible nitric oxide synthase and shows promise for treating non-alcoholic steatohepatitis (NASH). However, its poor water solubility and low bioavailability limits its clinical use. Here the drug was loaded into phosphatidylcholine-bile salt-mixed micelles (PBMM/SKLB023) to overcome these limitations.

**Methods:** PBMM/SKLB023 was developed using a simple co-precipitation method, and formulation parameters were optimized. The pharmacokinetics of PBMM/SKLB023 were investigated in Wistar rats, and therapeutic efficacy was assessed in a mouse model of NASH induced by a diet deficient in methionine- and choline.

**Results:** PBMM/SKLB023 particles were 11.36±2.08 nm based on dynamic light scattering, and loading the drug into micelles improved its water solubility 300-fold. PBMM/SKLB023 inhibited proliferation and activation of HSC-T6 cells more strongly than free SKLB023. PBMM/SKLB023 showed longer mean retention time and higher bioavailability than the free drug after intravenous injection in Wistar rats. In the mouse model of NASH, PBMM/SKLB023 alleviated hepatic lipid accumulation, inflammation, and fibrosis to a significantly greater extent than free SKLB023.

**Conclusion:** PBMM/SKLB023 shows therapeutic potential for treating NASH and liver fibrosis.

**Keywords:** phosphatidylcholine-bile salt-mixed micelles, bioavailability, solubilizing efficiency, NASH

## Introduction

Non-alcoholic steatohepatitis (NASH) is part of the spectrum of non-alcoholic fatty liver disease characterized by steatosis, inflammation, and progressive fibrosis.[1,2] Progression to NASH can ultimately result in severe and irreversible liver damage, including cirrhosis and hepatocellular carcinoma. NASH is typically accompanied by one or more metabolic disorders,[3] so slowing or halting NASH progression can help prevent severe liver diseases and metabolic disorders. There is no well-established pharmacological approach for treating NASH,[4,5] so studies aimed at exploring novel therapeutic agents to treat NASH are urgently needed.

The pathogenesis of NASH is complex,[6] and nitric oxide produced by inducible nitric oxide synthase (iNOS) plays an important role in its progression.[7,8] Reducing

Correspondence: Jinhan He
Laboratory of Clinical Pharmacy and Adverse Drug Reaction, State Key Laboratory of Biotherapy and Cancer Center, Collaborative Innovation Center of Biotherapy, West China Hospital of Sichuan University, No.37 Guoxue Alley, Wuhou District, Chengdu, Sichuan Province 610041, People's Republic of China
Tel +86 288 542 6416
Email jinhanhe@scu.edu.cn

submit your manuscript | www.dovepress.com
DovePress
http://doi.org/10.2147/IJN.S202821

iNOS expression improved insulin resistance and inflammation in mice on a high fat diet.[8,9] Therefore, inhibiting iNOS may help prevent fat accumulation and inflammation in the liver. Indeed, peroxisome proliferator-activated receptor-γ (PPAR-γ) down-regulates iNOS, and thiazolidinediones ligands of PPAR-γ exert anti-inflammatory effects.[10,11] Various natural and synthetic ligands of PPAR-γ inhibit the production of pro-inflammatory cytokines interleukin-1β (IL-1β) and tumor necrosis factor-α (TNF-α) in vitro.[12,13] A large, randomized, placebo-controlled trial of non-diabetic patients with NASH found that the thiazolidinedione pioglitazone significantly reduced steatosis, inflammation, hepatocyte ballooning, and levels of liver enzymes.[14]

These results encourage us to develop novel agents for the treatment of NASH and other inflammatory diseases related to nitric oxide and iNOS. We recently showed that the novel 5-benzylidenethiazolidine-2,4-dione based-derivative SKLB023 (Figure 1) reduced inflammation in rheumatoid arthritis,[15–17] and that it significantly attenuated hepatic lipid accumulation, inflammation, and fibrosis in NASH.[18] However, the aqueous solubility of SKLB023 was only 4 μg/mL, which limited the administration route to gavage. This route means low bioavailability and higher risk of unanticipated toxicity because of the higher doses needed to achieve a therapeutic effect.[15]

Here we addressed the poor water solubility and low bioavailability of SKLB023 by loading it into phosphatidylcholine-bile salt-mixed micelles (PBMM). These solubilizing micelles, which can be prepared using a simple co-precipitation method, are effective for rendering poorly soluble drugs suitable for intravenous administration.[19,20] Bile salts can solubilize phosphatidylcholine to form a clear solution of mixed micelles,[21] and solubilized phospholipids in the micelles can help neutralize the hemolytic effects of bile salts. PBMM can encapsulate drugs tightly and remain small enough (10–100 nm) for good pharmacokinetics and drug bioavailability. The mixed micelles are well tolerated locally and systemically, with no embryotoxic, teratogenic, or mutagenic effects after administration.[22]

We evaluated the ability of PBMM/SKLB023 to treat NASH in mice fed a diet deficient in methionine and choline. To our knowledge, this is the first SKLB023 nano-formulation to work well against NASH in an animal model.

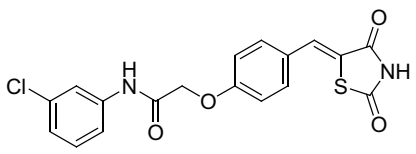


**Figure 1** Chemical structure of SKLB023.

# Materials and methods

## Materials and animals

SKLB023 was synthesized as described.[15] Egg phosphatidylcholine (EPC, 80% purity) was obtained from Lipoid GmbH (Ludwigshafen, Germany). Sodium glycocholate (SGC) was a gift from Chongqing Yaoyou Pharmaceutical (Chongqing, China). Tetrahydrofuran and other analytical grade chemicals were purchased from Sigma Aldrich (St. Louis, MO, USA). DMEM, penicillin, streptomycin, and fetal bovine serum were purchased from Hyclone (USA).

Animals were housed at West China Hospital, Sichuan University, in accordance

with the guidelines of the institutional Animal Care and Use Committee.

## Preparation and characterization of PBMM/SKLB023

Due to the good solubility of SKLB023, SGC, and EPC in tetrahydrofuran, SKLB023 was easily loaded into PBMM using the coprecipitation method.[23] Briefly, SKLB023, SGC, EPC at different molar ratios, and concentrations were dissolved in tetrahydrofuran, which was then evaporated at 40°C under vacuum to form a thin film. The film was rehydrated in physiological saline and dispersed by slight shaking, after which the pH was adjusted to approximately 7.4. To remove unloaded drug, the solution was centrifuged at 10,000 g for 10 minutes, and the supernatant containing PBMM was collected.

The single-factor method was used to optimize several factors in PBMM formulation, including the mass ratio of EPC and SGC, the total concentration of EPC and SGC, the dose of SKLB023 and the pH value of dispersed medium.

The particle size distribution and zeta-potential of PBMM/SKLB023 was determined by dynamic light scattering (Malvern Zetasizer Nano ZS90, Malvern Instruments Ltd, Malvern, UK). All results were the mean of three experiments. Morphology was examined using a transmission electron microscope (H-6009IV, Hitachi, Japan). The micellar solution was placed on copper grids, stained with 2% (w/v) phosphotungstic acid for 30 seconds, dried at room temperature, and examined.

## Drug solubility, solubilizing efficiency, and drug loading of PBMM/SKLB023

The concentration of the SKLB023 solubilized by PBMM was determined using high-performance liquid chromatography (HPLC), as described.[15] Measurements were the average of triplicate determinations. The solubilizing efficiency and drug loading (DL%) were calculated by the following equations:

$$\text{Solubilizing efficiently}(\%) = \text{weight of drug loaded} / \text{weight of drug input} \times 100\%$$

$$\text{DL}(\%) = \text{weight of drug loaded} / \text{total weight of micelles} \times 100\%$$

For the stability of PBMM/SKLB023, samples were stored at 4°C or 37°C for different periods of time, then the size and polydispersity index (PDI) were measured.

## Cell culture and treatment

Activated rat hepatic stellate cells HSC-T6 were cultured in DMEM with high glucose (Hyclone) supplemented with 10% FBS (Hyclone), 100 IU/mL penicillin, and 100 μg/mL streptomycin. Cells were maintained at 37°C in a humidified atmosphere containing 5% $CO_2$, and the culture medium was changed every other day.

For in vitro cytotoxicity, HSC-T6 cells were seeded in 96-well plates at a density of $5\times10^3$ per well and cultured at 37°C for 24 hours in the presence of 5% $CO_2$. Serial dilutions of blank PBMM, free SKLB023, or PBMM/SKLB023 in FBS-free medium were added to the wells, and plates were incubated for another 48 hours. Cytotoxicity of the different treatments against HSC-T6 cells was evaluated using the MTT assay.

For the in vitro anti-fibrosis assay, HSC-T6 cells were seeded in 6-well plates at a density of $4\times10^4$ per well and cultured at 37°C for 24 hours. Cells were treated with free SKLB023 or PBMM/SKLB023 (20 μmol/L) for 48 hours and then harvested.

## Pharmacokinetics in rats

Wistar rats (200±20 g) were randomly divided into two groups, with six rats in each group. SKLB023 or PBMM/SKLB023 were administered by intravenous injection through the tail vein at a dose of 10 mg/kg SKLB023. Blood was collected from the ocular vein into heparinized Eppendorf tubes at 5, 15, 30, 45, 60, 120, 240, and 300 minutes, then immediately centrifuged at 5,000 g at 4°C for 10 minutes. The supernatant was collected and stored at −80°C until analysis.

## Therapeutic effect of PBMM/SKLB023 in a mouse model of NASH

C57BL/6J mice were divided into four groups, with six mice in each group. Mice received a diet deficient in methionine and choline or the control amino acid diet (TrophicDiet, Nanchang, China) for 4 weeks. Then animals were treated with saline, SKLB023, or PBMM/SKLB023 daily by intravenous injection through the tail vein at a dose of 10 mg/kg SKLB023 for another 2 weeks, while being maintained on the deficient or control diet. At the end of 6 weeks, all mice were sacrificed, and samples of blood and liver were stored at −80°C for further analysis.

Liver function was assessed based on levels of serum alanine transaminase (ALT) and aspartate aminotransferase (AST), as assayed using appropriate commercial enzyme-based kits (Zhongsheng Technologies, Beijing, China) according to the manufacturer's instructions.

To analyze hepatic triglycerides levels, 150 mg of liver was homogenized in 1 mL of phosphate-buffered saline (PBS). Total lipids were extracted using chloroform/methanol (2:1, v/v) and dissolved in 1% Triton X-100 in ethanol. Triglycerides were measured using commercial kits (Zhongsheng Technologies).

For histological analysis, livers were fixed in 4% formaldehyde, embedded in paraffin, sectioned to a thickness of 5 μm, and stained with hematoxylin and eosin. Frozen sections (10 μm) were used for Oil Red O staining.

## Quantitative RT-PCR

Total cellular RNA was extracted with Trizol reagent and reverse-transcribed into cDNA using the iScript cDNA synthesis kit (TaKaRa, Kyoto, Japan). Quantitative real-time PCR was performed using the SYBR green-based assay with CFX96 Real-Time system (Bio-rad, Hercules, CA, USA). The following primer sequences was used (shown 5'-3'): α-SMA sense, CTGTGCTATGTCGCTCTGGA; α-SMA anti-sense, ATAGGTGGTTTCGTGGATGC; Col1a1 sense, GGTCAGACCTGTGTGTTCCC; Col1a1 anti-sense, GGTCCATGTAGGCTACGCTG; TGF-β sense, GCTAATGGTGGACCGCAACAA; TGF-β anti-sense, CACTGCTTCCCGAA

TGTCTGA; PAI-1 sense, CCGAGAGCTTTGTGA AGGAG; and PAI-1anti-sense, ACATCTGCATCCT GGAGCTT.

## Statistical analysis

Results are expressed as the mean±SEM for each sample. Statistical significance was determined using Student's unpaired two-tailed *t*-test or one-way ANOVA for multiple comparisons with Tukey's test. $P<0.05$ was considered statistically significant.

# Results

## Solubilizing efficiency of different PBMM/SKLB023 formulations

The influence of the mass ratio EPC to SGC on solubilizing efficiency of PBMM/SKLB023 at a constant SKLB023 concentration of 1.0 mg/mL was examined (Figure 2A). When the ratio decreased from 1:0.7 to 1:1.5, the efficiency of SKLB023 solubilization increase significantly. However, a further decrease of the ratio from 1:1.5 to 1:2 slightly reduced the solubilizing efficiency. Thus, a ratio of 1:1.5 was used in subsequent studies, providing solubilizing efficiencies as high as 98.25%.

While keeping the SKLB023 concentration at 1.0 mg/kg, the influence of total concentration of EPC and SGC on solubilizing efficiency was investigated (Figure 2B). The efficiency was maximal at a total concentration of 50 mg/mL, and it did not increase further when the total concentration rose above 50 mg/mL.

SKLB023 concentration influenced the stability of PBMM (Table 1). The maximal concentration was around 1.0 mg/mL, with higher concentrations destabilizing the micelles.

The influence of pH on the solubilizing efficiency of PBMM/SKLB023 was examined (Figure 2C). Increasing pH between the range of 2 and 8 dramatically improved solubilizing efficiency, which slightly decreased at pH values higher than 8. At physiological pH around 7.4, solubilizing efficiency was as high as 95.45%, so this value was used in subsequent experiments.

The results of this single-factor optimization led us to formulate PBMM/SKLB023 using 1.0 mg SKLB023, 20 mg EPC, 30 mg SGC, and 1.0 mL physiological saline.

## Characterization of PBMM/SKLB023

The solubility of SKLB023 in water was approximately 0.0032 mg/mL, which increased to 0.98±0.02 mg/mL after loading into PBMM based on the optimized formulation.

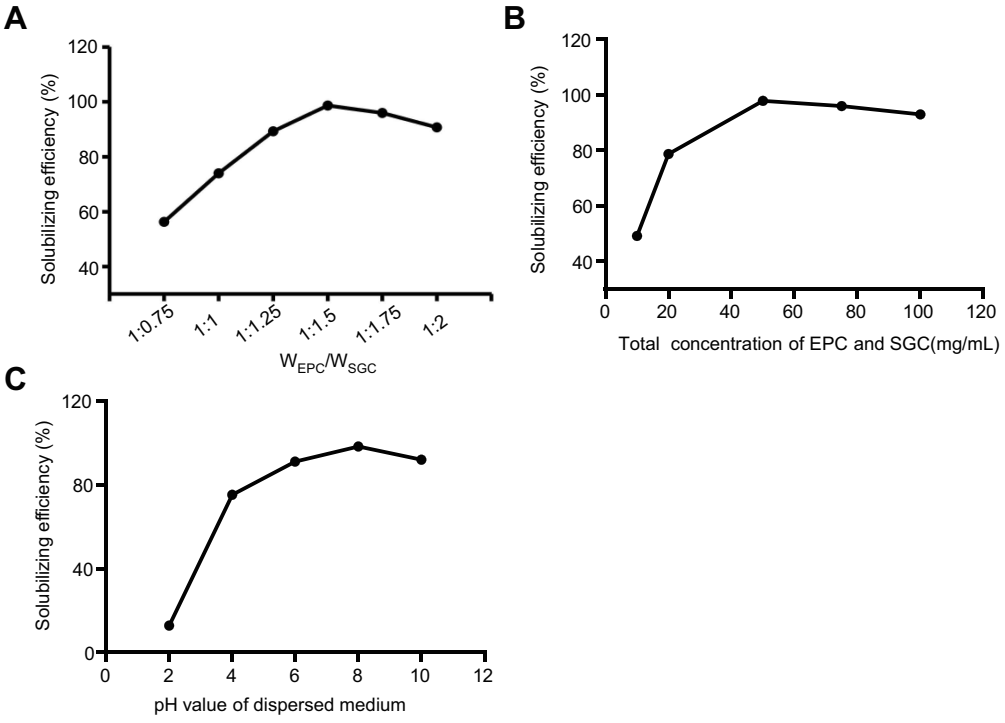


**Figure 2** (**A**) Influence of mass ratio of egg phosphatidylcholine (EPC) and sodium glycocholate (SGC) on SKLB023 solubilizing efficiency at 25°C (n=3). (**B**) Influence of total concentration of SGC and EPC on SKLB023 solubilizing efficiency at 25°C (n=3). (**C**) Influence of pH value of the dispersing medium on SKLB023 solubilizing effciency at 25°C (n=3).

**Table 1** Influence of SKLB023 concentration on the stability of PBMM/SKLB023

| SKLB023 (mg/mL) | EPC+SGC (mg) | Time (h) | | | |
|---|---|---|---|---|---|
| | | 0 | 1 | 8 | 24 |
| 0.25 | 50 | Y | Y | Y | Y |
| 0.50 | 50 | Y | Y | Y | Y |
| 1.0 | 50 | Y | Y | Y | Y |
| 1.5 | 50 | Y | Y | C | C |
| 2.0 | 50 | C | C | C | C |

**Notes:** Y represents settled solution; C represents SKLB023 separating out; n=3.

Solubilizing efficiency of PBMM/SKLB023 was 98.26% ±1.45%, while drug loading efficiency was 1.92%±0.12% (Table 2).

Figure 3A illustrates the structures of PBMMB/SKLB023. Based on three separate measurements, the mean size of PBMM/SKLB023 was 11.36±2.08 nm, with a polydispersity index of 0.12±0.02, and the zeta-potential was −6.8±1.2 mV (Figures 3B and C). Transmission electron microscopy showed that micelles were spherical, homogeneous, and monodisperse (Figure 3D).

The average size of PBMM/SKLB023 remained nearly unchanged for 7 days at both 4°C and 37°C, and polydispersity index increased only slightly over the same period (Figures 3E and F). These results suggested the good stability of PBMM/SKLB023.

## Anti-fibrosis effect of PBMM/SKLB023 on HSC-T6 cells

Since activation and proliferation of hepatic stellate cells (HSCs) is key in progression of NASH-related liver fibrosis,[24,25] the activated HSC cell line HSC-T6 was used to investigate the efficacy of PBMM/SKLB023 in vitro. After 48-hours treatment with various concentrations of blank PBMM, the viability in the MTT assay was >90%, suggesting low cytotoxicity (Figure 4A). PBMM/SKLB023 significantly inhibited HSC-T6 proliferation, and it inhibited proliferation to a greater extent than free SKLB023.

**Table 2** Solubilizing efficiency and drug loading of PBMM/SKLB023

| | Solubility (mg/mL) | Solubilizing efficiency (%) | Drug loading (%) |
|---|---|---|---|
| PBMM/SKLB023 | 0.98±0.02 | 98.26%±1.45% | 1.92%±0.12% |

**Notes:** Data reported as mean±standard deviation; n=3.

Next we compared free SKLB023 and PBMM/SKLB023 for their ability to inhibit fibrosis in HSC-T6 cells, based on quantitative PCR analysis of four fibrosis-related genes (α-SMA, Col1a1, TGF-β, and PAI-1). At the same concentration of 20 μmol/L, free SKLB023 showed a negligible effect on mRNA levels of these genes, whereas PBMM/SKLB023 dramatically reduced them. This may reflect the greater uptake of PBMM/SKLB023 than free drug into cells. These results indicated that PBMM/SKLB023 can effectively inhibit HSC-T6 proliferation and activation.

## Pharmacokinetics

Plasma concentrations of SKLB023 over time in rats injected with PBMM/SKLB023 or free SKLB023 are shown in Figure 5. Levels of PBMM/SKLB023 were significantly higher than those of free SKLB023 at all time points, and PBMM/SKLB023 showed longer clearance time from plasma (Table 3). PBMM/SKLB023 was associated with significantly higher $C_{max}$ (52.03±5.65 mg/L) than free SKLB023 (9.54±1.30 mg/L), longer $t_{1/2}$ (0.74 vs 0.37 h) and 6.04-fold greater $AUC_{0-t}$. These encouraging results suggest that PBMM/SKLB023 can increase the therapeutic efficacy of SKLB023.

## PBMM/SKLB023 can alleviates steatosis in a mouse model

To assess the therapeutic efficacy of PBMM/SKLB023 against NASH in an animal model, we fed mice with a control diet or a diet deficient in methionine and choline for 6 weeks. This deficient diet is widely used to induce key features of NASH, including steatosis, hepatic inflammation, and fibrosis.[26,27] Alanine aminotransferase (ALT) and aspartate aminotransferase (AST) serve as surrogate markers of liver injury. As expected, the deficient diet significantly increased serum levels of ALT and AST as well as hepatic levels of triglycerides (Figure 6). These increases were suppressed by free SKLB023 and PBMM/SKLB023, while the nanoparticle formulation showed significantly greater therapeutic effect than the free drug.

Histology examination also provided supportive evidence for the results obtained from the biochemical analysis. Mice on the deficient diet showed obvious vesicular lesions and severe neutrophile infiltration, and this was moderately improved after treatment with free SKLB023, but substantially improved after treatment with PBMM/SKLB023 (Figure 6D). Consistently, PBMM/SKLB023 reduced the number and size of fat droplets more than free SKLB023, based on Oil Red

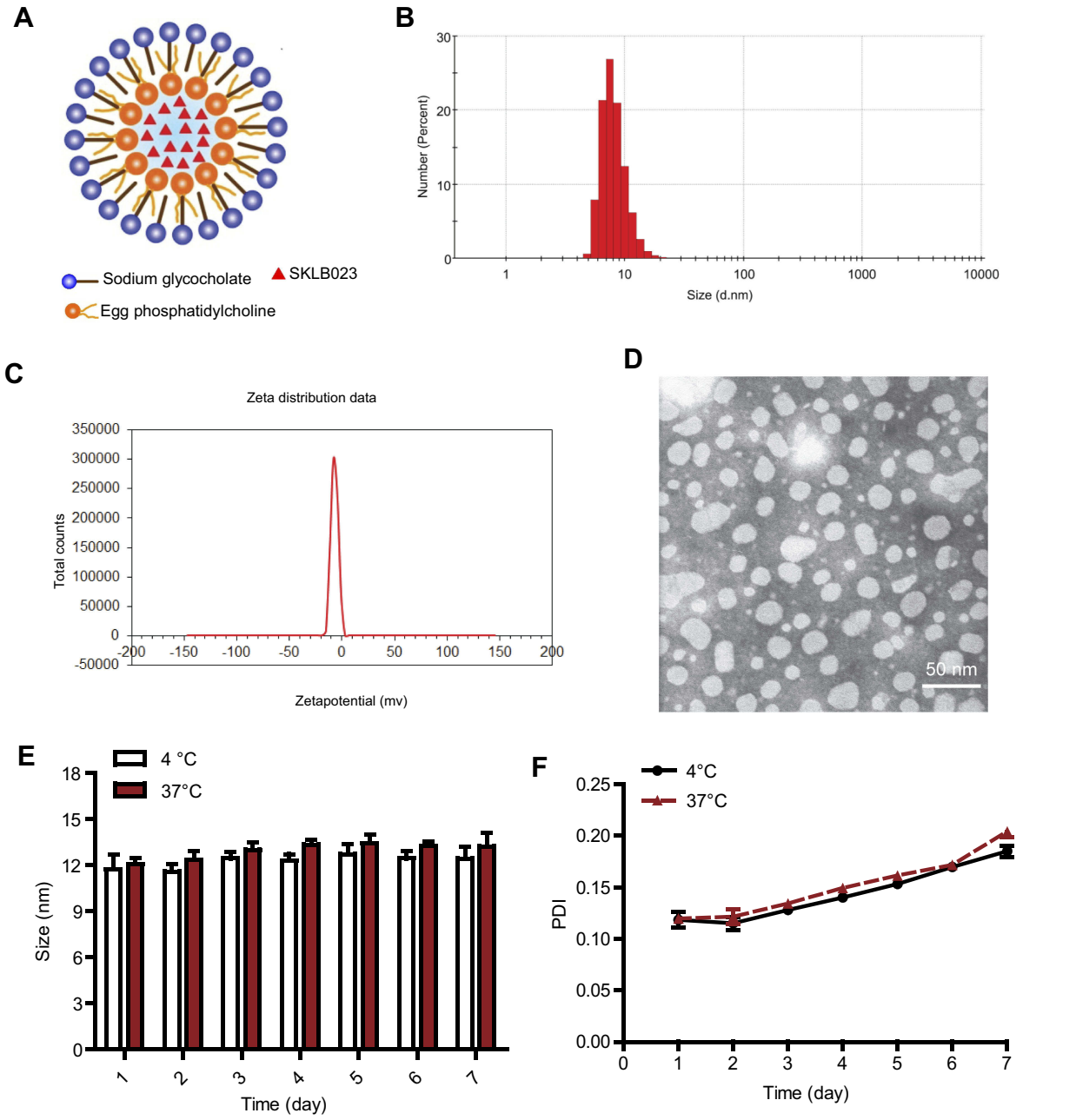


**Figure 3** Characterization of PBMM/SKLB023 micelles. (**A**) Schematic illustration of PBMM/SKLB023 micelles. (**B**) Particle size. (**C**) zeta-potential distribution. (**D**) Transmission electron micrograph. (**E**) Particle size. (**F**) polydispersity index of PBMM/SKLB023 micelles at 4°C or 37°C for 7 days.

O staining (Figure 6E). These results suggest greater therapeutic effects with PBMM/SKLB023 than with free SKLB023. Notably, PBMM/SKLB023 showed comparable effects with pioglitazone (Figure S1), a well documented drug active on NASH.[28–30]

## PBMM/SKLB023 can alleviate liver fibrosis and inflammation in a mouse model

Liver fibrosis was assessed using Sirius red and Masson's trichrome staining. Liver tissue from mice on a deficient diet stained positive for collagen (Figures 7A and B), which moderately improved after treatment with free SKLB023, but substantially improved after treatment with PBMM/SKLB023.

The deficient diet stimulated inflammatory response, based on quantitative PCR analysis of levels of mRNAs expressing the proinflammatory factors TNF-α, IL-6, IL-1β, MCP-1, and PAI-1 (Figure 7C). As in the histology analyses, free SKLB023 significantly reduced these levels, but PBMM/SKLB023 reduced them to an even greater extent. These results suggest that PBMM/SKLB023 is

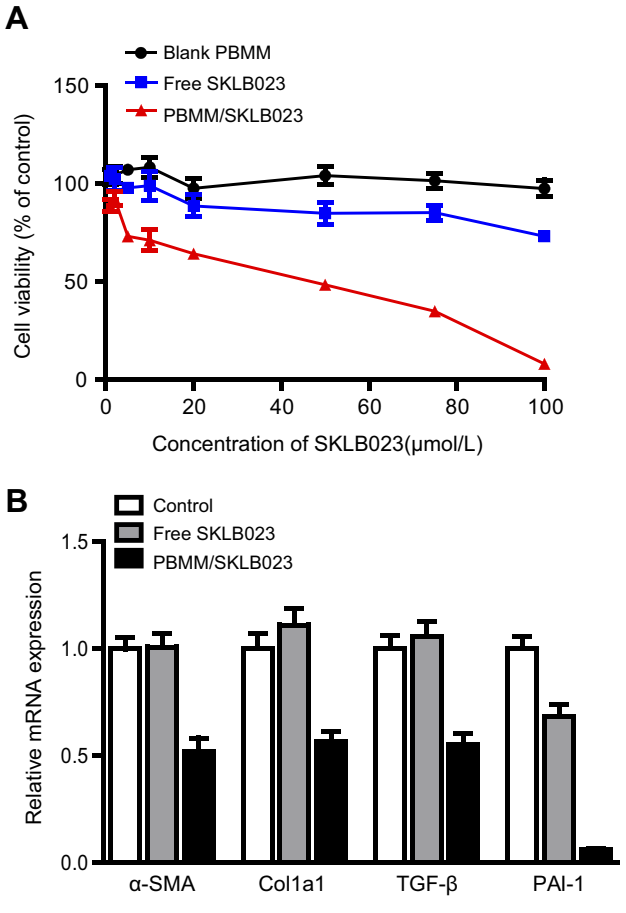


**Figure 4** Anti-fibrosis effects of PBMM/SKLB023 in vitro. (**A**) Viability of HSC-T6 cells treated with different formulations. Data are mean±SD (n=5). (**B**) Relative mRNA levels of fibrosis-related genes (α-SMA, Col1a1, TGF-β, and PAI-1) in HSC-T6 cells treated with different formulations. Data are mean±SD (n=3).

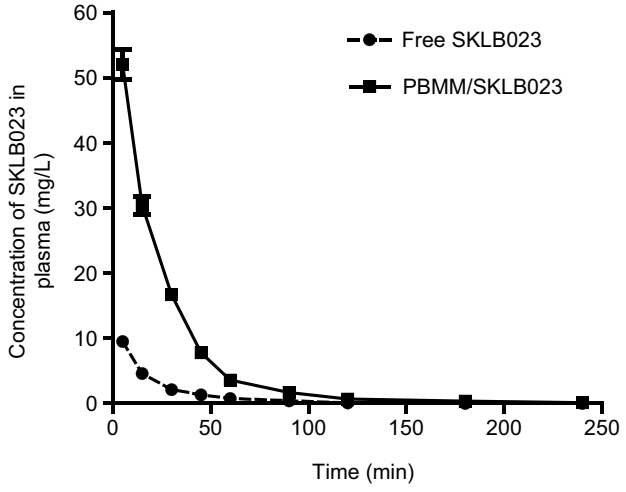


**Figure 5** Mean plasma concentration-time curves after intravenous administration of SKLB023 and PBMM/SKLB023 in Wistar rats. In both conditions, the equivalent dose was 10 mg/kg.

superior to free drug for alleviating liver fibrosis and hepatic inflammation in a mouse model of NASH.

**Table 3** The main pharmacokinetic parameters of the free SKLB023 and PBMM/SKLB023 in rats

| Parameter | Free SKLB023 | PBMM/SKLB023 |
|---|---|---|
| $AUC_{0-t}$ (mg/L*h) | 4.13±0.60 | 24.96±1.66 |
| $MRT_{0-t}$ (h) | 0.26±0.02 | 0.43±0.03 |
| $t_{1/2}$ (h) | 0.37±0.06 | 0.74±0.10 |
| $C_{max}$ (mg/L) | 9.54±1.30 | 52.03±5.65 |

**Notes:** Data reported as mean±standard deviation; n=6.
**Abbreviations:** AUC, area under the curve; MRT, mean retention time.

## Discussion

There is no established treatment for NASH, which is becoming a major public health issue and is a leading cause of liver transplantation.[31,32] Numerous clinical studies have demonstrated that thiazolidinediones can significantly improve steatosis, inflammation, hepatocyte ballooning, and levels of liver enzymes in NASH with advanced fibrosis.[14,33] Thiazolidinediones work at least in part by inhibiting the activity of the proinflammatory factors NF-κB, iNOS, and IL-6.[12]

In our previous study, we demonstrated that the novel 5-benzylidenethiazolidine-2,4-dione based-derivative SKLB023 showed potent effects against hepatic lipid accumulation, inflammatory, and fibrosis in a mouse model of NASH induced by a diet deficient in methionine and choline.[15,18] However, the aqueous solubility of SKLB023 was only 4 μg/mL, which limited the administration route to gavage, leading to low bioavailability. In the present study, we increased drug efficacy by loading it into a phosphatidylcholine-bile salts-mixed micelle system that can facilitate the drug's delivery to all organs, avoiding the absorption process. Such micelles have proven similarly effective with other drugs targeting other diseases.[19,23,34] To our knowledge, this is the first SKLB023 nano-formulation to show efficacy against NASH.

In order to optimize the PBMM/SKLB023 preparation, we examined how water solubility and drug loading efficiency depended on three main solubilization parameters: (1) EPC/SGC mass ratio, (2) total concentration of EPC and SGC, and (3) pH value. Following optimization of these parameters, we obtained spherical particles of 11 nm with a zeta potential of −7 mV, and they behaved as a stable, uniform system. The aqueous solublity of SKLB023 in PBMM was 0.98 mg/mL, approximately 300-fold higher than that of free SKLB023 (0.0032 mg/mL).

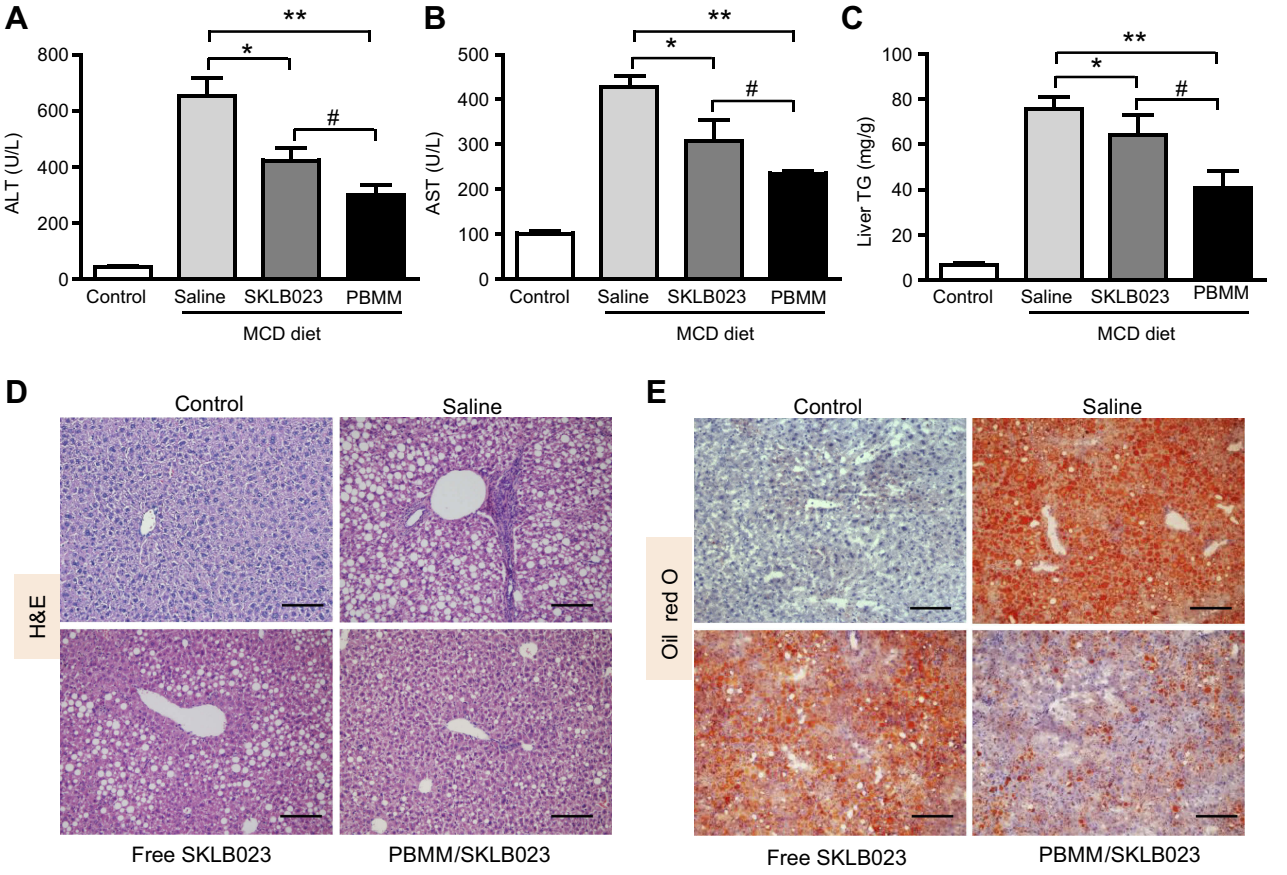


**Figure 6** Therapeutic efficacy of PBMM/SKLB023 in a mouse model of NASH induced with a diet deficient in methionine and choline (MCD diet). Animals treated with free SKLB023 or PBMM/SKLB023 were assessed for (**A**) Serum alanine aminotransferase (ALT), (**B**) serum aspartate aminotransferase (AST), and (**C**) hepatic triglyceride (TG). Liver sections of mice were stained with (**D**) hematoxylin-eosin (H&E) or (**E**) Oil Red O. Scale bar, 100 μm. *$P$<0.05 and **$P$<0.01 vs saline-treated NASH animals, #$P$<0.05 vs free SKLB023 (n=6 for each group).

Pharmacokinetic studies showed that $C_{max}$ and mean retention time of SKLB023 in plasma were significantly greater when the drug was delivered in PBMM/SKLB023, resulting in a 6-fold higher AUC than for the free drug. These results are likely due to interactions between the drug and PBMM when the mixed micelles are above the critical micelle concentration at the time of administration.[19,35] The bile salts and phospholipid in the mixed micelles may also help the uptake of SKLB023 into organ tissue.

We found that PBMM/SKLB023 showed greater anti-fibrosis activity than free SKLB023 in vitro and in vivo. PBMM/SKLB023 was superior to free drug in inhibiting the proliferation and activation of hepatic stellate cells HSC-T6, as well as protecting a NASH mouse model against liver injury, lipid accumulation, inflammatory and hepatic fibrosis. The efficacy-enhancing ability of PBMM may involve multiple mechanisms. Two have been discussed above: the ability of PBMM micelles to solubilize SKLB023 in the circulation, which translates to greater bioavailability in plasma, and to increase drug uptake into cells, since cells can endocytose nanoparticles. A third mechanism may be that damage to blood vessels in fibrotic liver can enhance delivery of mixed micelles to the tissue through the enhanced permeability and retention effect (EPR), analogous to the situation with solid tumors.[36–38]

## Conclusions

Formulating the weakly water-soluble drug SKLB023 into mixed micelles based on phosphatidylcholine and bile salts substantially improved its solubility and, therefore, its bioavailability following intravenous injection. The stable, uniform particles were better than free SKLB023 at alleviating hepatic lipid accumulation, inflammation, and fibrosis in a mouse model of NASH induced by a diet deficient in methionine and choline. These results,

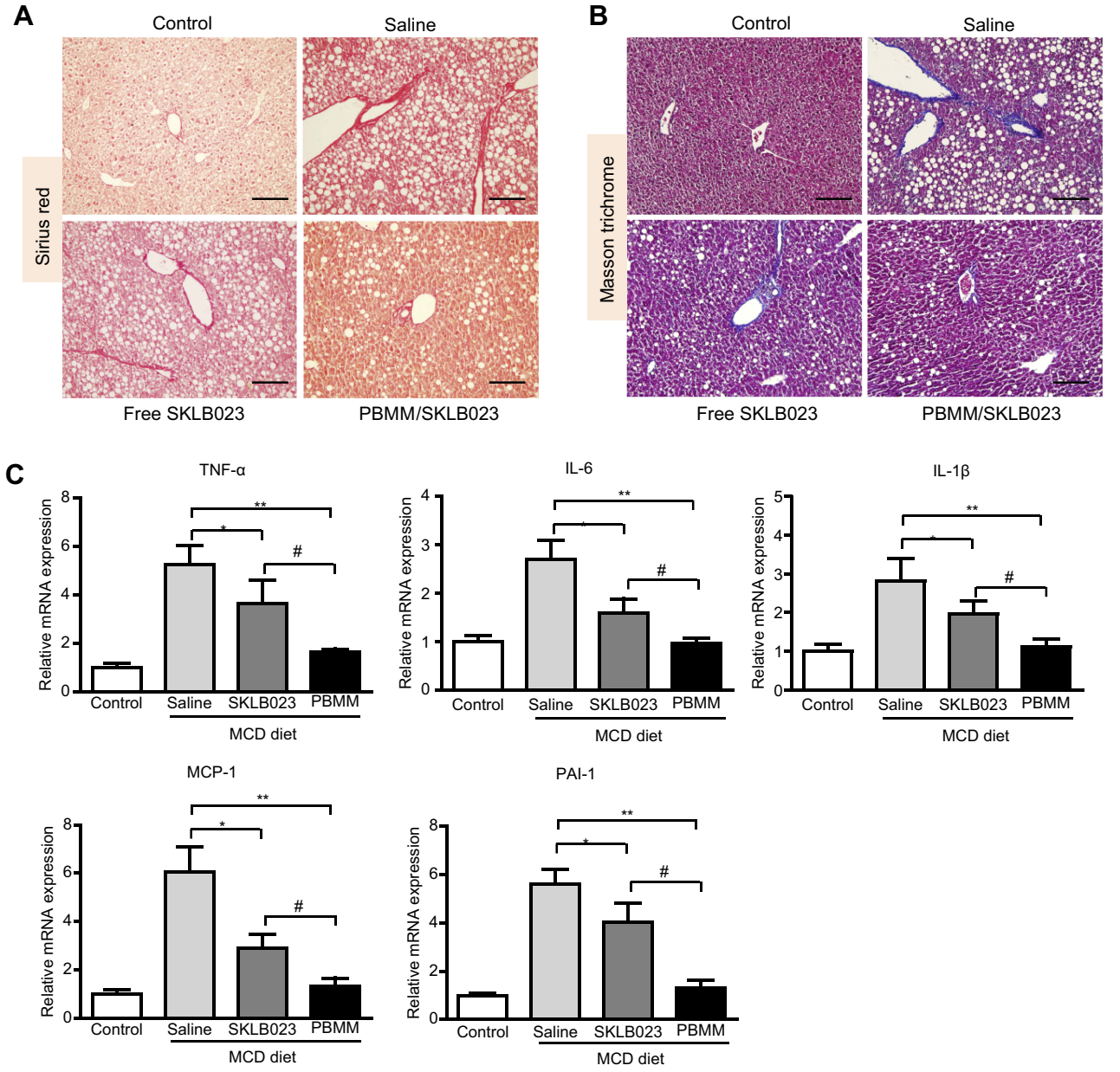


**Figure 7** Anti-fibrosis efficacy of PBMM/SKLB023 in a mouse model of NASH induced with a diet deficient in choline and methionine (MCD diet). Liver tissue from mice after treatment with different formulations was stained with (**A**) Sirius Red or (**B**) Masson trichrome. Scale bar: 100 μm. (**C**) Liver tissue was homogenized and assayed for relative levels of mRNAs expressing TNF-α, IL-6, IL-1β, MCP-1, and PAI-1. *$P$<0.05 and **$P$<0.01 vs saline-treated NASH animals, #$P$<0.05 vs free SKLB023 (n=6 for each group).

together with the potentially simple scale-up of PBMM/SKLB023 production, suggest therapeutic potential against NASH and liver fibrosis.

## Acknowledgments

This work was financially supported by the National Natural Science Foundation of China (81603035 and 81870599), and China Postdoctoral Fellowship (2017M612981 and 2018T110986).

## Disclosure

The authors report no conflicts of interest in this work.

## References

1. Younossi ZM. Non-alcoholic fatty liver disease-a global public health perspective. *J Hepatol*. 2019;70(3):531–544. doi:10.1002/hep.30251
2. Byass P. The global burden of liver disease: a challenge for methods and for public health. *BMC Med*. 2014;12:159. doi:10.1186/s12916-014-0141-2
3. Younossi Z, Tacke F, Arrese M, et al. Global perspectives on non-alcoholic fatty liver disease and non-alcoholic steatohepatitis. *Hepatology*. 2018. doi:10.1002/hep.30251

4. Takahashi Y, Sugimoto K, Inui H, Fukusato T. Current pharmacological therapies for nonalcoholic fatty liver disease/nonalcoholic steatohepatitis. *World J Gastroenterol*. 2015;21(13):3777–3785. doi:10.3748/wjg.v21.i10.2937
5. Noureddin M, Zhang A, Loomba R. Promising therapies for treatment of nonalcoholic steatohepatitis. *Expert Opin Emerg Drugs*. 2016;21(3):343–357. doi:10.1080/14728214.2016.1220533
6. Milic S, Mikolasevic I, Krznaric-Zrnic I, et al. Nonalcoholic steatohepatitis: emerging targeted therapies to optimize treatment options. *Drug Des Devel Ther*. 2015;9:4835–4845. doi:10.2147/DDDT.S64877
7. Aram G, Potter JJ, Liu X, Torbenson MS, Mezey E. Lack of inducible nitric oxide synthase leads to increased hepatic apoptosis and decreased fibrosis in mice after chronic carbon tetrachloride administration. *Hepatology (Baltimore, Md*. 2008;47(6):2051–2058. doi:10.1002/hep.22149
8. Iwakiri Y. Nitric oxide in liver fibrosis: the role of inducible nitric oxide synthase. *Clin Mol Hepatol*. 2015;21(4):319–325. doi:10.3350/cmh.2015.21.4.319
9. Anavi S, Eisenberg-Bord M, Hahn-Obercyger M, Genin O, Pines M, Tirosh O. The role of iNOS in cholesterol-induced liver fibrosis. *Lab Invest*. 2015;95(8):914–924. doi:10.1038/labinvest.2015.67
10. Yasmin S, Jayaprakash V. Thiazolidinediones and PPAR orchestra as antidiabetic agents: from past to present. *Eur J Med Chem*. 2017;126:879–893. doi:10.1016/j.ejmech.2016.12.020
11. Tacelli M, Celsa C, Magro B, et al. Antidiabetic drugs in NAFLD: the accomplishment of two goals at once?. *Pharmaceuticals (Basel)*. 2018;11(4):121.
12. Ye Y, Lin Y, Manickavasagam S, Perez-Polo JR, Tieu BC, Birnbaum Y. Pioglitazone protects the myocardium against ischemia-reperfusion injury in eNOS and iNOS knockout mice. *Am J Physiol Heart Circ Physiol*. 2008;295(6):H2436–H2446. doi:10.1152/ajpheart.00017.2008
13. Youssef J, Badr MZ. PPARs: history and advances. *Methods Mol Biol*. 2013;952:1–6.
14. Musso G, Cassader M, Paschetta E, Gambino R. Thiazolidinediones and advanced liver fibrosis in nonalcoholic steatohepatitis: a meta-analysis. *JAMA Intern Med*. 2017;177(5):633–640. doi:10.1001/jamainternmed.2016.9607
15. Ma L, Xie C, Ma Y, et al. Synthesis and biological evaluation of novel 5-benzylidenethiazolidine-2,4-dione derivatives for the treatment of inflammatory diseases. *J Med Chem*. 2011;54(7):2060–2068. doi:10.1021/jm1011534
16. Xie C, Ma L, Liu J, et al. SKLB023 blocks joint inflammation and cartilage destruction in arthritis models via suppression of nuclear factor-kappa B activation in macrophage. *PLoS One*. 2013;8(2):e56349. doi:10.1371/journal.pone.0056349
17. Feng Y, Xu J, Guo F, et al. SKLB023 hinders renal interstitial fibrosis in obstructive nephropathy by interfering TGF-β1/Smad3 signaling. *RSC Adv*. 2018;8(11):5891–5896. doi:10.1039/C8RA00018B
18. Zhang J, Li Y, Liu Q, et al. SKLB023 as an iNOS inhibitor alleviated liver fibrosis by inhibiting the TGF-beta/Smad signaling pathway. *RSC Adv*. 2018;8(54):30919–30924. doi:10.1039/C8RA04955F
19. Duan RL, Sun X, Liu J, Gong T, Zhang ZR. Mixed micelles loaded with silybin-polyene phosphatidylcholine complex improve drug solubility. *Acta Pharmacol Sin*. 2011;32(1):108–115. doi:10.1038/aps.2010.209
20. Hammad MA, Muller BW. Increasing drug solubility by means of bile salt-phosphatidylcholine-based mixed micelles. *Eur J Pharm Biopharm*. 1998;46(3):361–367. doi:10.1016/S0939-6411(98)00037-X
21. Hammad MA, Muller BW. Solubility and stability of tetrazepam in mixed micelles. *Eur J Pharm Sci*. 1998;7(1):49–55. doi:10.1016/S0928-0987(98)00006-2
22. Teelmann K, Schlappi B, Schupbach M, Kistler A. Preclinical safety evaluation of intravenously administered mixed micelles. *Arzneimittel-Forschung*. 1984;34(11):1517–1523.
23. Song X, Jiang Y, Ren C, et al. Nimodipine-loaded mixed micelles: formulation, compatibility, pharmacokinetics, and vascular irritability study. *Int J Nanomedicine*. 2012;7:3689–3699. doi:10.2147/IJN.S30631
24. Higashi T, Friedman SL, Hoshida Y. Hepatic stellate cells as key target in liver fibrosis. *Adv Drug Deliv Rev*. 2017;121:27–42. doi:10.1016/j.addr.2017.05.007
25. Tsuchida T, Friedman SL. Mechanisms of hepatic stellate cell activation. *Nat Rev Gastroenterol Hepatol*. 2017;14(7):397–411. doi:10.1038/nrgastro.2017.38
26. Zamin I Jr., Mattos AA, Mattos AZ, Migon E, Soares E, Perry ML. Model of experimental nonalcoholic steatohepatitis from use of methionine and choline deficient diet. *Arq Gastroenterol*. 2009;46(1):69–74. doi:10.1590/S0004-28032009000100017
27. He J, Hu B, Shi X, et al. Activation of the aryl hydrocarbon receptor sensitizes mice to nonalcoholic steatohepatitis by deactivating mitochondrial sirtuin deacetylase Sirt3. *Mol Cell Biol*. 2013;33(10):2047–2055. doi:10.1128/MCB.00646-12
28. Uto H, Nakanishi C, Ido A, et al. The peroxisome proliferator-activated receptor-gamma agonist, pioglitazone, inhibits fat accumulation and fibrosis in the livers of rats fed a choline-deficient, l-amino acid-defined diet. *Hepatol Res*. 2005;32(4):235–242.
29. Serfaty L. Pioglitazone: the beginning of a new era for NASH? *J Hepatol*. 2007;47(1):160–162. doi:10.1016/j.jhep.2007.03.002
30. Kalavalapalli S, Bril F, Koelmel JP, et al. Pioglitazone improves hepatic mitochondrial function in a mouse model of nonalcoholic steatohepatitis. *Am J Physiol Endocrinol Metab*. 2018;315(2):E163–e173. doi:10.1152/ajpendo.00023.2018
31. Marra F, Gastaldelli A, Svegliati Baroni G, Tell G, Tiribelli C. Molecular basis and mechanisms of progression of non-alcoholic steatohepatitis. *Trends Mol Med*. 2008;14(2):72–81. doi:10.1016/j.molmed.2007.12.003
32. Satapathy SK, Sanyal AJ. Novel treatment modalities for nonalcoholic steatohepatitis. *Trends Endocrinol Metab*. 2010;21(11):668–675. doi:10.1016/j.tem.2010.08.003
33. Rotman Y, Sanyal AJ. Current and upcoming pharmacotherapy for non-alcoholic fatty liver disease. *Gut*. 2017;66(1):180–190. doi:10.1136/gutjnl-2016-312431
34. Guo Q, Cai J, Li P, et al. Comparison of bile salt/phosphatidylcholine mixed micelles in solubilization to sterols and stability. *Drug Des Devel Ther*. 2016;10:3789–3798. doi:10.2147/DDDT.S119918
35. Dongowski G, Fritzsch B, Giessler J, Hartl A, Kuhlmann O, Neubert RH. The influence of bile salts and mixed micelles on the pharmacokinetics of quinine in rabbits. *Eur J Pharm Biopharm*. 2005;60(1):147–151. doi:10.1016/j.ejpb.2005.01.003
36. Jiménez Calvente C, Sehgal A, Popov Y, et al. Specific hepatic delivery of procollagen α1(I) small interfering RNA in lipid-like nanoparticles resolves liver fibrosis. *Hepatology (Baltimore, Md*. 2015;62(4):1285–1297. doi:10.1002/hep.27936
37. Zhang S, Wu J, Wang H, et al. Liposomal oxymatrine in hepatic fibrosis treatment: formulation, in vitro and in vivo assessment. *AAPS PharmSciTech*. 2014;15(3):620–629. doi:10.1208/s12249-014-0086-y
38. Peer D, Karp JM, Hong S, Farokhzad OC, Margalit R, Langer R. Nanocarriers as an emerging platform for cancer therapy. *Nat Nanotechnol*. 2007;2(12):751–760. doi:10.1038/nnano.2007.387